

Single-molecule transistor fabrication by self-aligned lithography and in situ molecular assembly

J. Tang ^{a,d}, E.P. De Poortere ^{b,d}, J.E. Klare ^{a,d}, C. Nuckolls ^{a,d}, S.J. Wind ^{c,d,*}

^a Department of Chemistry, Columbia University, New York, NY 10027, USA

^b Department of Physics, Columbia University, New York, NY 10027, USA

^c Department of Applied Physics and Applied Mathematics, Columbia University, New York, NY 10027, USA

^d Center for Electron Transport in Molecular Nanostructures, Columbia University, New York, NY 10027, USA

Available online 21 February 2006

Abstract

We describe the fabrication of single-molecule transistors by self-aligned lithography and in situ molecular assembly. Ultrathin metallic electrodes are patterned with a nanoscale interelectrode separation defined by the lateral oxidation of a thin layer of Al. Highly conjugated molecular units are sequentially assembled within the electrode gap by selective design of the molecular end group chemistry. The assembled devices display evidence of molecular conduction.

© 2006 Elsevier B.V. All rights reserved.

Keywords: Nanolithography; Molecular electronics; Molecular self-assembly

1. Introduction

A primary goal of the field of molecular electronics is the realization of electronic switches comprising individual molecules as the key functional unit [1]. These devices represent the ultimate in field-effect transistor scaling [2]. The study of their electronic transport properties can provide a detailed understanding of electron dynamics at the nanoscale and will help determine whether or not such devices are technologically feasible.

Highly conjugated organic molecules synthesized for such studies are no more than a few nanometers in length, and the reliable fabrication of electrodes that can be bridged by a single molecule remains a significant challenge.

In this work, we have developed two new techniques for the fabrication and assembly of single-molecule transistors. The first technique involves the patterning of metallic electrodes separated by a nanoscale gap into which a single

molecule may be inserted. The electrode fabrication technique is self-aligned, requiring no extraordinary lithographic capabilities. It is nonetheless capable of producing sub-10 nm gaps with very high yield. Control of the interelectrode separation is determined by the oxidation of a thin sacrificial layer of Al, which is deposited directly upon the first electrode.

The second technique involves the in situ assembly of the molecule within the gap. The assembly is based upon the ability to chemically distinguish between the three critical interfaces in the device: metal/molecule; molecule/molecule; and molecule/dielectric. This is done by functionalizing individual molecular units with appropriate end-groups, such that they will selectively attach either to the metallic electrodes, to the gate dielectric or to other individual molecular units. By assembling the molecules in this way, a given device may be designed with specific chemical or electrical functionality. In addition, the length of the molecule may be modified by this in situ assembly, relaxing the requirement that the molecule “fit” precisely in the interelectrode gap, thus making it easier to wire up conjugated molecules.

* Corresponding author.

E-mail address: sw2128@columbia.edu (S.J. Wind).

2. Electrode fabrication

The critical steps for the self-aligned fabrication of the nanoelectrodes, shown schematically in Fig. 1, involves two separate lithographic patterning steps. Only gross ($\sim\mu\text{m}$ scale) alignment is required between the two steps, as nanoscale precision is achieved by a self-aligned process.

Samples are fabricated on heavily doped (n-type) Si substrates upon which a thin layer ($\sim 4\text{--}7\text{ nm}$) of ZrO_2 has been deposited by atomic layer deposition. The substrate serves as a gate electrode [3,4], and the ZrO_2 is the gate dielectric. Because of the high dielectric constant of ZrO_2 ($\sim 20\text{--}24$), thicker films may be used relative to SiO_2 , while achieving the same effective gate field coupling. ZrO_2 provides an additional advantage when Pt is used as the electrode material, in that Pt grows on ZrO_2 in two-dimensional sheets [5,6], leading to extremely smooth Pt films which are conductive even at thicknesses of only a few nm.

The first step in the nanoelectrode formation process is lithographic patterning of the first electrode. This is done by electron beam lithography, although virtually any lithographic method may be used. A sample is coated with a layer of PMMA (poly-methylmethacrylate), to a thickness ranging from ~ 25 to 120 nm , depending on the thickness of the metal to be deposited. Exposure of the first electrode pattern is done in an FEI Sirion scanning electron microscope equipped with a pattern generator and control system from J.C. Naby, Inc. The first electrode pattern typically consists of a rectangle with dimensions $\sim 1\text{ }\mu\text{m}$ or less on a side. This enables easy alignment of the second electrode pattern in a subsequent lithographic exposure.

Following exposure and PMMA development, a Pt film with thickness of less than $\sim 5\text{ nm}$ is deposited by electron beam evaporation, followed by a layer of Al, which is deposited in situ directly after the Pt. The Al film thickness is typically $\sim 5\text{--}30\text{ nm}$, as determined by a quartz crystal microbalance. After removal from the electron beam evaporator, the sample undergoes liftoff in a mixture of CH_2Cl_2 and acetone (9:1) at 75°C . The first electrode pattern covered by the Al film is shown schematically in Fig. 1a. Al oxidizes easily in air and is known to form a robust native

oxide layer with thickness of a few nm [7] (Fig. 1b). (It may be possible to oxidize the Al film in situ prior to removal of the sample from the electron beam evaporator. This may afford improved control over the thickness of the Al.) Because of the thinness of the Al layer, it has been somewhat difficult to determine the precise thickness of the oxide layer by standard ellipsometric and scanning electron microscope techniques [7], although efforts continue to further characterize these films via high resolution transmission electron microscopy (TEM).

The second electrode is patterned by electron beam lithography using a process similar to the first electrode patterning. The pattern is coarsely aligned to the first electrode using pre-patterned alignment marks. The second electrode pattern consists of rectangles similar to those in the first electrode pattern, although they may be narrower in one dimension, in order to limit the number of molecules that will assemble between the electrodes. (In this work, the second electrode width is chosen to be $\sim 20\text{ nm}$.) The narrow second electrode pattern runs across the first electrode, as in Fig. 1c. The electron channel of the transistor will be formed at the intersection of the two rectangles.

Following exposure and development of the second electrode pattern, a second metal film is deposited by electron beam evaporation. The metal may be the same as the first electrode material, or it may be different. For this work, we have chosen to form the second electrode from Pt. The thickness of the second electrode is critical. It cannot be substantially thicker than the first electrode, as it will tend to form on the sidewall of the Al film, making it difficult to remove when the Al is stripped. After the second electrode metal deposition, the sample undergoes another liftoff step similar to that used for the first electrode patterning. This leaves a narrow strip of metal running across the first electrode.

At this point in the process, the Al is removed by immersion in an etchant solution. Depending on the materials used, the etchant can be either acid or base. In the case of Pt on ZrO_2 , the Al is removed in an aqueous solution of TMAH (tetramethylammoniumhydroxide), followed by a H_2O rinse. This step removes the Al and Al_2O_3 and the second layer of metal which was patterned on top of the first electrode, as shown in Fig. 1d. A narrow gap is formed between the two electrodes, as shown in Fig. 2 for two different thicknesses of deposited Al. As the Al is oxidized, the oxide grows both vertically and laterally. If the extent of the lateral oxidation is a function of the deposited Al thickness, it will allow for the “tuning” of the interelectrode gap by controlling the thickness of the Al and its oxidation.

The yield of this process in terms of the number of devices on a sample with nanometer-spaced electrodes as a function of devices patterned is extremely high, $\sim 80\%$. Devices which fail are typically those for which the second metal is not cleanly removed when the Al is stripped, leaving “shorts” between the two electrodes. Thus, as mentioned above, the thickness of the second electrode metal

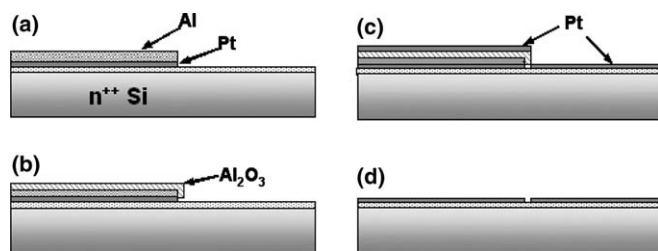


Fig. 1. Nanogap fabrication sequence. (a) First electrode is patterned. A bilayer consisting of the first electrode metal (Pt) and a thin layer of Al is lifted off. (b) The Al is allowed to oxidize in air. (c) A second lithography and deposition step defines the second electrode (Pt). (d) The Al is stripped, leaving the two metal electrodes separated by a nanogap.

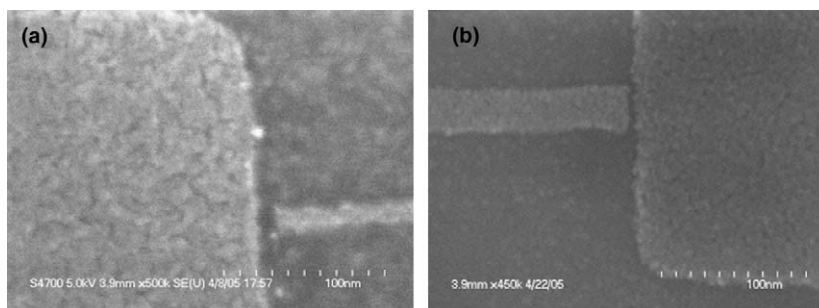


Fig. 2. Pt (~ 4 nm thick) nanogaps on ZrO_2 fabricated by the technique shown in Fig. 1. (a) 10 nm gap (30 nm Al) and (b) 5 nm gap (8 nm Al).

must be carefully controlled so as not to exceed the thickness of the first electrode.

Although the electrodes are quite thin (only a few nm), they have been found to be quite conductive, with sheet resistances of $\sim 10^3 \Omega/\square$. In order to minimize total series resistance, macroscopic pads and leads are patterned by either optical lithography or electron beam lithography. The metal thickness of these pads and leads is ~ 50 – 100 nm.

3. Molecular assembly

The molecule used in this work is formed from cruciform π -systems that have a terphenyl arm that is crossed with a conjugated bisoxazole arm [8]. The molecule can be functionalized with a variety of reactive endgroup chemistries [8], enabling its attachment to other organic molecules or its assembly in ordered monolayers on metal surfaces [9]. Since the molecule is only ~ 2.3 nm long, it is assembled in the interelectrode gap in two steps, as shown schematically in Fig. 3. The device is first soaked in a solution of the bisoxazole molecule which has been functionalized to assemble on the Pt electrodes (molecule a in Fig. 3). This is followed by attachment of the molecule (molecule b in Fig. 3) functionalized to connect to the free ends of the previously assembled units, thereby bridging the interelectrode gap. Details of the chemical assembly will be provided in a separate publication [10].

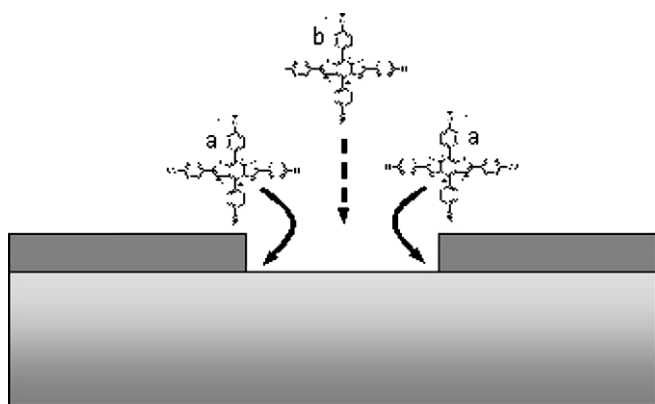


Fig. 3. Modular assembly of bis-oxazole molecule in a nanogap. Monothiol-terminated molecule (a) is attached to the electrodes, followed by attachment of diamine-terminated molecule (b).

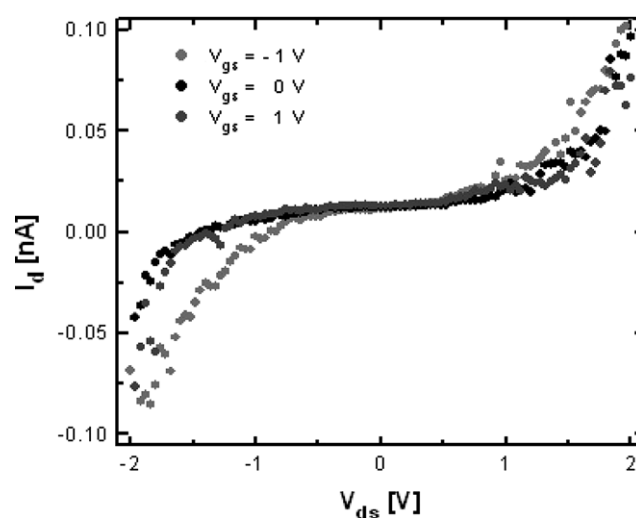


Fig. 4. Room temperature output characteristics for an assembled bis-oxazole molecule in a 4-nm gap device. The gate dielectric was 1 nm SiO_2 and 3.7 nm ZrO_2 .

4. Electrical results

Electrical probing of devices following the first step shows no significant current. However, following the second reaction, a distinctive tunneling current with a magnitude up to \sim a few nA is measured with bias voltages up to 2 V at room temperature, as shown in Fig. 4. The gate voltage is switched between -1 and $+1$ V. Gate field modulation appears to be weak in this range. This may be due to inefficient gate coupling to the molecule and/or possibly to the need for increased gate potential in order to effect noticeable shifting of the molecular energy levels relative to the Fermi level of the metal electrodes. Further experiments will investigate this issue as well as the behavior of these devices at low temperature.

5. Conclusions

We have demonstrated a new method for fabricating electrodes for probing single molecules. The method is completely self-aligned, relying upon the oxidation of a thin layer of Al to determine the size of the interelectrode gap. Using in situ assembly of molecules between these

electrodes, we observe electron transport through these molecules.

Acknowledgments

This work was supported primarily by the Nanoscale Science and Engineering Initiative of the National Science Foundation under NSF Award Number CHE-0117752 and by the New York State Office of Science, Technology, and Academic Research (NYSTAR).

References

- [1] A. Aviram, M.A. Ratner, *Chem. Phys. Lett.* 29 (1974) 277–283.
- [2] V.V. Zhirnov, R.K. Cavin, J.A. Hutchby, G.I. Bourianoff, *Proc. IEEE* 91 (2003) 1934–1939.
- [3] S.J. Tans, A.R.M. Verschueren, C. Dekker, *Nature* 393 (1998) 49–52.
- [4] R. Martel, T. Schmidt, H.R. Shea, T. Hertel, P. Avouris, *Appl. Phys. Lett.* 73 (1998) 2447–2449.
- [5] S. Roberts, R.J. Gorte, *J. Phys. Chem.* 95 (1991) 5600–5604.
- [6] P.A. Dilara, J.M. Vohs, *J. Phys. Chem.* 99 (1995) 17259–17264.
- [7] A. Bachtold, P. Hadley, T. Nakanishi, C. Dekker, *Science* 294 (2001) 1317–1320.
- [8] J.E. Klare, G.S. Tulevski, K. Sugo, A. de Picciotto, K.A. White, C. Nuckolls, *J. Am. Chem. Soc.* 125 (2003) 6030–6031.
- [9] J.E. Klare, G.S. Tulevski, C. Nuckolls, *Langmuir* 20 (2004) 10068–10072.
- [10] J.E. Klare, J. Tang, S.J. Wind, C. Nuckolls, in preparation.